Anal. Chem. **2009,** *81,* 875–882

Synthesis of Fluorescent Carbohydrate-Protected Au Nanodots for Detection of Concanavalin A and *Escherichia coli*

Chih-Ching Huang,[†] Chao-Tsen Chen,[‡] Yen-Chun Shiang,[‡] Zong-Hong Lin,[‡] and Huan-Tsung Chang*[,‡]

Institute of Bioscience and Biotechnology, National Taiwan Ocean University, Keelung, Taiwan, and Department of Chemistry, National Taiwan University, Taipei, Taiwan

Downloaded by NATIONAL TAIWAN UNIV on July 30, 2009
Published on January 2, 2009 on http://pubs.acs.org | doi: 10.1021/ac8010654

This study describes a novel, simple, and convenient method for the preparation of water-soluble biofunctional Au nanodots (Au NDs) for the detection of Concanavalin A (Con A) and *Escherichia coli* (*E. coli*). First, 2.9 nm Au nanoparticles (Au NPs) were prepared through reduction of $HAuCl_4 \cdot 3H_2O$ with tetrakis(hydroxymethyl)phosphonium chloride (THPC), which acts as both a reducing and capping agent. Addition of 11-mercapto-3,6,9-trioxaundecyl-α-D-mannopyranoside (Man-SH) onto the surfaces of the as-prepared Au NPs yielded the fluorescent mannose-protected Au nanodots (Man-Au NDs) with the size and quantum yield (QY) of 1.8 (±0.3) nm and 8.6%, respectively. This QY is higher than those of the best currently available water-soluble, alkanethiol-protected Au nanoclusters. Our fluorescent Man-Au NDs are easily purified and by multivalent interactions are capable of sensing, under optimal conditions, Con A with high sensitivity (LOD = 75 pM) and remarkable selectivity over other proteins and lectins. To the best of our knowledge, this approach provided the lowest LOD value for Con A when compared to the other nanomaterials-based detecting method. Furthermore, we have also developed a new method for fluorescence detection of *E. coli* using these water-soluble Man-Au NDs. Incubation with *E. coli* revealed that the Man-Au NDs bind to the bacteria, yielding brightly fluorescent cell clusters. The relationship between the fluorescence signal and the *E. coli* concentration was linear from 1.00×10^6 to 5.00×10^7 cells/mL ($R^2 = 0.96$), with the LOD of *E. coli* being 7.20×10^5 cells/mL.

Semiconductive and metallic nanomaterials exhibiting quantized properties have become the focus of new applications in optoelectronics, catalysis, and medical diagnostics.[1] With unique optical properties, sizes similar to those of biopolymers, and large surface areas, nanoparticles (NPs) and quantum dots (QDs) conjugated with biomolecules have attracted great interest for cell imaging and the sensing of molecules of interest in biological samples.[1] Carbohydrate-modified metallic NPs, magnetic NPs and QDs have been used to explore carbohydrate−protein interactions,[2] which, on cell surfaces, play key roles in many cellular processes, including cell growth regulation, differentiation, immune response, cellular trafficking, adhesion, cancer cell metastasis, and inflammation by bacteria and viruses.[3,4] Proteins possessing carbohydrate-binding domains are known as lectins.[4]

Carbohydrate−protein interactions are generally weak, but they can be compensated for by the presentation of multiple ligands to their respective binding proteins.[3] One approach is to assemble many carbohydrate units onto the surfaces of NPs; the resulting polyvalent interactions between the multiple ligands and proteins can be collectively much stronger than that of the corresponding monovalent interaction.[2] The shift in the surface plasmon absorption band and the consequent color change associated with the aggregation of carbohydrate-stabilized metallic NPs has led to the development of colorimetric assays for selectively sensing lectins.[5] Carbohydrate−QD conjugates have also been developed to study protein−carbohydrate interactions.[6] Concerns have been raised, however, regarding the toxicity of QDs; several studies have suggested that the cytotoxicity of QDs

* To whom correspondence should be addressed. Professor Huan-Tsung Chang, Department of Chemistry, National Taiwan University, 1, Section 4, Roosevelt Road, Taipei 106, Taiwan. Phone and fax: 011-886-2-33661171. E-mail: changht@ntu.edu.tw.

[†] National Taiwan Ocean University.

[‡] National Taiwan University.

(1) (a) Salgueiriño-Maceira, V.; Correa-Duarte, M. A. *Adv. Mater.* **2007**, *19*, 4131–4144. (b) Haick, H. *J. Phys. D: Appl. Phys.* **2007**, *40*, 7173–7186. (c) Huang, X.; Jain, P. K.; El-Sayed, I. H.; El-Sayed, M. A. *Nanomedicine* **2007**, *2*, 681–693. (d) Medintz, I. L.; Uyeda, H. T.; Goldman, E. R.; Mattoussi, H. *Nat. Mater.* **2005**, *4*, 435–446. (e) Jamiesona, T.; Bakhshia, R.; Petrova, D.; Pococka, R.; Imani, M.; Seifalian, A. M. *Biomaterials* **2007**, *28*, 4717–4732.

(2) (a) de la Fuente, J. M.; Penadés, S. *Biochim. Biophys. Acta* **2006**, *1760*, 636–651. (b) El-Boubbou, K.; Gruden, C.; Huang, X. *J. Am. Chem. Soc.* **2007**, *129*, 13392–13393.

(3) (a) Jelinek, R.; Kolusheva, S. *Chem. Rev.* **2004**, *104*, 5987–6015. (b) de la Fuente, J. M.; Penadés, S. *Glycoconjugate J.* **2004**, *21*, 149–163. (c) Dwek, R. A. *Chem. Rev.* **1996**, *96*, 683–720. (d) Simanek, E. E.; McGarvey, G. J.; Jablonowski, J. A.; Wong, C.-H. *Chem. Rev.* **1998**, *98*, 833–862.

(4) Lis, H.; Sharon, N. *Chem. Rev.* **1998**, *98*, 637–674.

(5) (a) Schofield, C. L.; Haines, A. H.; Field, R. A.; Russell, D. A. *Langmuir* **2006**, *22*, 6707–6711. (b) Otsuka, H.; Akiyama, Y.; Nagasaki, Y.; Kataoka, K. *J. Am. Chem. Soc.* **2001**, *123*, 8226–8230. (c) Takae, S.; Akiyama, Y.; Otsuka, H.; Nakamura, T.; Nagasaki, Y.; Kataoka, K. *Biomacromolecules* **2005**, *6*, 818–824. (d) Hone, D. C.; Haines, A. H.; Russell, D. A. *Langmuir* **2003**, *19*, 7141–7144.

(6) (a) Chen, Y.; Ji, T.; Rosenzweig, Z. *Nano Lett.* **2003**, *3*, 581–584. (b) Sun, X.-L.; Cui, W.; Haller, C.; Chaikof, E. L. *ChemBioChem* **2004**, *5*, 1593–1596. (c) Babu, P.; Sinha, S.; Surolia, A. *Bioconjugate Chem.* **2007**, *18*, 146–151.

10.1021/ac8010654 CCC: $40.75 © 2009 American Chemical Society
Published on Web 01/02/2009

Scheme 1. Schematic Representation of the Preparation of Fluorescent Man-Au NDs for the Detection of Con A and *E. coli*

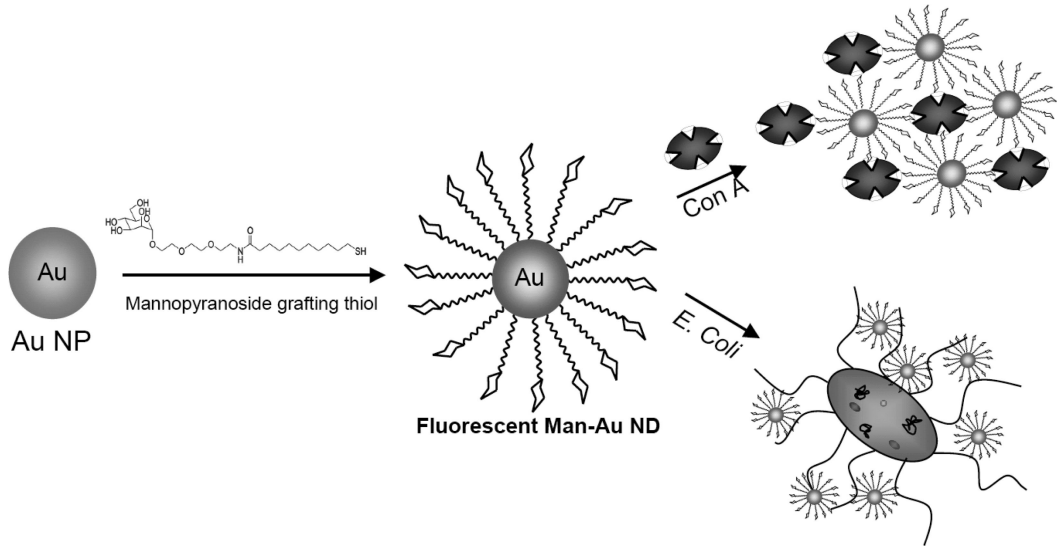

Downloaded by NATIONAL TAIWAN UNIV on July 30, 2009
Published on January 2, 2009 on http://pubs.acs.org | doi: 10.1021/ac8010654

might be mediated by their release of Cd^{2+}.[7] Thus, there is a demand for the development of nontoxic fluorescent NPs to replace potentially toxic QDs in bioassays. Although multivalent forms of carbohydrate-functionalized fluorescent polymers have been employed to successfully detect lectins and to label bacteria, there are problems associated with their water solubility and complicated syntheses in organic phases.[8] Here, we report a universal, simple, and convenient method for the preparation of water-soluble, luminescent, α-D-mannose-conjugated Au nanodots (Man-Au NDs) and demonstrate their applications to detection of concanavalin A (Con A) and *Escherichia coli* (*E. coli*) through multivalent cooperative interactions between Man-Au NDs and proteins (Scheme 1).

EXPERIMENTAL SECTION

Chemicals. Mannose, glucose, galactose, lactose, tetrakis(hydroxymethyl)phosphonium chloride (THPC), and all of the metal salts used in this study were purchased from Aldrich (Milwaukee, WI). All proteins and lectins were obtained from Sigma (St. Louis, MO). Sodium tetraborate and hydrogen tetrachloroaurate(III) trihydrate were obtained from Acros (Geel, Belgium). All of the other salts and buffers were purchased from Aldrich. 11-Mercapto-3,6,9-trioxaundecyl-α-D-mannopyranoside was synthesized and purified according to previously reported procedures.[9]

Synthesis of Au NPs. The Au NPs were synthesized through reduction of $HAuCl_4 \cdot 3H_2O$ with THPC.[10,11] A THPC solution (1 mL), which had been prepared by mixing 80% THPC solution (12 μL) with water (1 mL), was added to a solution formed by mixing 1 M NaOH (0.5 mL; Aldrich) with water (45 mL). The mixture was stirred for 5 min, followed by the rapid addition of 1 wt % $HAuCl_4 \cdot 3H_2O$ (1.34 mL). The color of the solution turned brown over the course of 1 min. The solution was stirred for 15 min and then stored at 4 °C prior to further use. The average size of the as-prepared Au NPs was determined using transmission electron microscope (Tecnai 20 G2 S-Twin TEM, Philips/FEI, Hillsboro, Oregon) to be 2.9 (±0.5) nm. The particle concentration of the as-prepared Au NP solution was determined to be 0.94 μM by using the equation ($n = 3m/4\pi r^3 s$), assuming the presence of ideal spherical particles, in which n is the amount of gold particles per milliliter, m is the molar mass of gold in the substance [g/mL], r is the particle radius [cm], and s is the specific gravity of colloidal gold [19.3 g/cm^3].[12] The m and r values were determined by conducting inductively coupled plasma mass spectroscopy (ICP-MS) and TEM measurements, respectively. This formula gives the number of Au NP per milliliter. This concentration was then converted into number of gold particles per liter and divided by Avogadro's number (6.023×10^{23}) to get the final molar concentration of gold nanoparticles.

Preparation of Fluorescent Man-Au NDs. The Man-Au NDs were prepared from the as-prepared Au NPs (0.47 μM) using Man-SH (40 mM). The as-prepared Au NP solution (5.0 mL), DI water (3.375 mL), trisodium tetraborate (50 mM, pH 9.2, 1.0 mL), and Man-SH (0.625 mL, 40 mM) were added sequentially into a 10 mL volumetric flask. The mixture was left to react for 72 h in the dark at room temperature. The resulting Man-Au NDs exhibited fluorescence. We further prepared different sizes of Man-Au NDs by varying the molar ratios of Man-SH to Au NPs (the concentrations of Man-SH were over the range 0−20 mM, while that of Au NPs was 0.46 μM). We purified the fluorescent Man-Au NDs by conducting centrifugal filtration (13 500*g*) for 40 min through a filter having a cutoff of 10 kDa (membrane nominal pore size ~1 nm). We then washed the pellets with 5 mM sodium phosphate (pH 7.0) several times. Most of the Man-SH, precursors, and possibly Au (I)-thiolate in the solution were removed. We then measured the fluorescence of the removed solution, showing a very weak fluorescence when excited at 375 nm. By comparison of the absorbance of the original Man-Au NDs solution at 375

(7) Hardman, R. *Environ. Health Persp.* **2006**, *114*, 165–172.
(8) (a) Disney, M. D.; Zheng, J.; Swager, T. M.; Seeberger, P. H. *J. Am. Chem. Soc.* **2004**, *126*, 13343–13346. (b) Xue, C.; Jog, S. P.; Murthy, P.; Liu, H. *Biomacromolecules* **2006**, *7*, 2470–2474.
(9) Tsai, C.-S.; Yu, T.-B.; Chen, C.-T. *Chem. Commun.* **2005**, 4273–4275.
(10) Huang, C.-C.; Yang, Z.; Lee, K.-H.; Chang, H.-T. *Angew. Chem., Int. Ed.* **2007**, *46*, 6824–6828.
(11) Duff, D. G.; Baiker, A.; Edwards, P. P. *Langmuir* **1993**, *9*, 2301–2309.
(12) Ackerman, G. A.; Yang, J.; Wolken, K. W. *J. Histochem. Cytochem.* **1983**, *31*, 433–440.

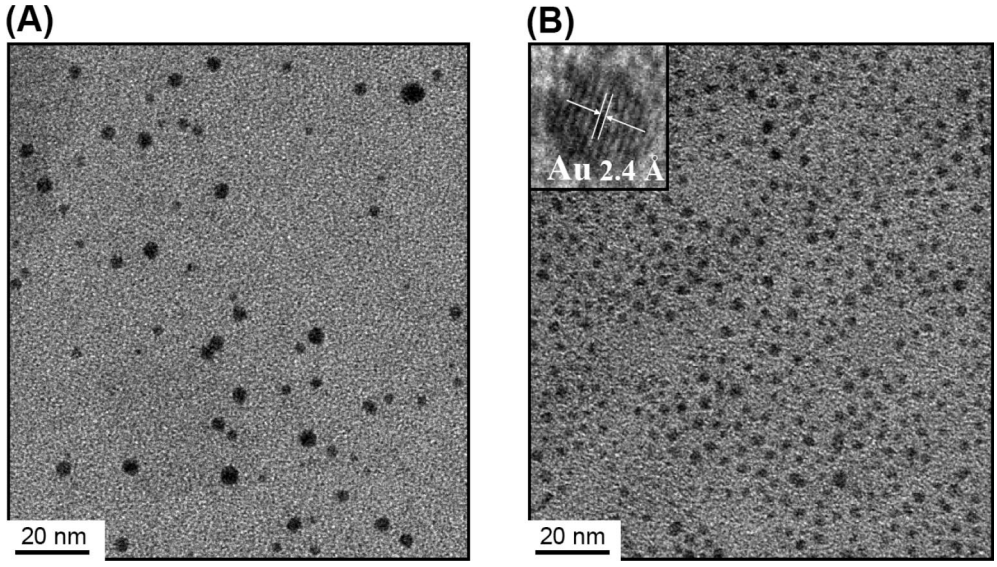

Figure 1. TEM images of the (A) Au NPs and (B) Man-Au NDs. The inset to part B is an HRTEM image of a Man-Au ND.

Downloaded by NATIONAL TAIWAN UNIV on July 30, 2009
Published on January 2, 2009 on http://pubs.acs.org | doi: 10.1021/ac8010654

nm to that of the resuspended solution, ~95% of the Man-Au NDs was deemed to have been collected (data not shown). On the other hand, the suspended solution fluoresced more strongly, which reveals that the fluorescence signal is truly from the particles. The corresponding particle concentration in the resuspended solution was estimated to be 1.5 μM, provided that the Man-Au NDs had a uniform diameter of 1.8 (±0.3) nm, which was estimated from a count of 100 Man-Au NDs particles in a transmission electron microscopy (TEM) image. The purified Man-Au ND sample was stable for at least 2 months when stored at 4 °C in the dark. Energy-dispersive X-ray spectroscopy (EDS) analysis using a 0.7 nm diameter electron probe was employed to determine the chemical identities of the Man-Au NDs. The measurement was conducted by illuminating an electron beam on a whole ND. The absorption and fluorescence spectra of the as-prepared Man-Au ND solutions were measured using a Cintra 10e UV−vis spectrometer (GBC, Victoria, Australia) and a Cary Eclipse fluorescence spectrophotometer (Varian, CA), respectively.

Turn-On Fluorescence Assays of Con A. A series of mixtures (1.0 mL) of Con A (0−10.0 nM) and Man-Au NDs (1.0 nM) in a buffer solution (10 mM sodium phosphate, 0.1 mM $MnCl_2$, and 0.1 mM $CaCl_2$; pH 7.0) were equilibrated at room temperature for 60 min. Subsequently, the mixtures were centrifuged (RCF 20 000*g*, 20 min) and the supernatants were removed. The precipitates were resuspended in a buffer (pH 7.0, 100 μL) containing 10 mM sodium phosphate, 0.1 mM $MnCl_2$, 0.1 mM $CaCl_2$, and 100 mM mannose, and then they were left to stand for another 60 min. All solutions were then transferred into 0.4 mL quartz cuvettes; their fluorescence spectra were measured by operating the fluorescence spectrophotometer at an excitation wavelength of 375 nm.

Bacterial Growth and Assays. *E. coli* K12 wild-type strains (ATCC 25404) were grown in sterile Luria−Bertani (LB) media [containing bacto-tryptone (2.5 g), bacto-yeast extract (1.25 g), and NaCl (2.5 g) in 250 mL of deionized water adjusted to pH to 7.0 with 5.0 M NaOH]. A single colony of each strain was lifted from agar plates and inoculated in LB media (10 mL), and the culture was grown overnight until the value of A_{600} reached 1.0. A portion of each of the cell mixtures (1 mL) was centrifuged (10 000*g*, 20 min, 4 °C) and washed twice with PBS buffer (100 mM Na_2HPO_4, 1.75 mM KH_2PO_4, 140 mM NaCl, and 2.70 mM KCl; adjusted to pH 7.4 using HCl; 1 mL). The washed cells were resuspended in PBS buffer (1.0 mL) containing $CaCl_2$ (0.1 mM) and $MnCl_2$ (0.1 mM). Cells diluted to $(1.00 \times 10^6)-(2.50 \times 10^8)$ cells/mL were incubated with the Man-Au NDs (25 nM) for 60 min under gentle shaking, centrifuged (10 000*g*, 20 min), and washed twice with PBS buffer; the final cell pellets were resuspended in PBS buffer containing 100 mM mannose.

RESULTS AND DISCUSSION

Preparation of Man-AuNDs. We prepared Man-Au NDs from 2.9 (±0.5) nm Au NPs (Figure 1A) in an aqueous phase at room temperature using Man-SH. First, we prepared the Au NPs through reduction of $HAuCl_4 \cdot 3H_2O$ with THPC, which acts as both a reducing and capping agent (Figure 1). Addition of Man-SH onto the surfaces of the as-prepared Au NPs yielded the fluorescent Man-Au NDs. TEM revealed that the as-prepared Man-Au NDs were spherical, having diameters of 1.8 (±0.3) nm (Figure 1B); i.e., the diameters of the spherical particles decreased upon being capped with Man-SH. This phenomenon is presumably due to the formation of the very strongly covalent, distinctly directional Au−S bonds and the preference for dissociation into very small Au and Au-thiolate clusters (on the basis of fragmentation energies), as opposed to breaking the Au−S bonds and detaching the Au clusters from the thiolate radical.[13] The inset in Figure 1B (high-resolution transmission electron microscope (HRTEM) image) suggests that the lattice fringes of the as-prepared Man-Au NDs are consistent with metallic gold having a discerned lattice spacing of 2.4 Å, which corresponds to the d-spacing of the (111) crystal plane of fcc Au.[14] EDS measurements were conducted to confirm the presence of the Man-SH molecules at the surface of the Au NDs. The EDS spectrum of the Man-Au NDs shown in Figure S1 in the Supporting Information indicates the presence of Au from the Au NDs and also C, O, and S from the Man-SH

(13) (a) Krüger, D.; Fuchs, H.; Rousseau, R.; Marx, D.; Parrinello, M. *J. Chem. Phys.* **2001**, *115*, 4776–4786. (b) Konôpka, M.; Rousseau, R.; Štich, I.; Marx, D. *J. Am. Chem. Soc.* **2004**, *126*, 12103–12111.
(14) Buffat, P.-A.; Flüeli, M.; Spycher, R.; Stadelmann, P.; Borel, J.-P. *Faraday Discuss.* **1991**, *92*, 173–187.

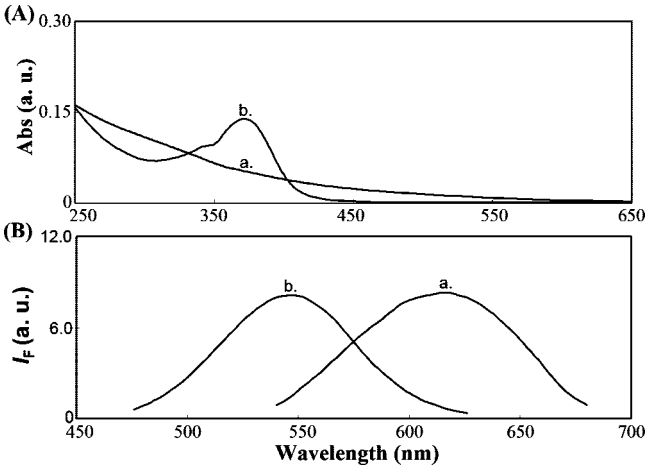

Figure 2. (A) UV−vis absorbance and (B) normalized fluorescence spectra of (a) Au NPs and (b) Man-Au NDs. The fluorescence intensities are plotted in arbitrary units (au); excitation wavelength: 375 nm. In part B, the ratio of the concentrations of the Au NPs and Man-Au NDs was 240 000: 1.

Downloaded by NATIONAL TAIWAN UNIV on July 30, 2009
Published on January 2, 2009 on http://pubs.acs.org | doi: 10.1021/ac8010654

molecules. The Cu peaks are due to the copper grid used in the sample preparation. The large sulfur peak evident in the EDS spectrum confirms an existence of a significant amount of Man-SH molecule at the surface of the Au NDs; the ratio of S/Au was determined to be 0.79 ± 0.4 (n = 5) from S K and Au L lines.

Optical Properties and Stability of Man-AuNDs. Although the Man-Au NDs exhibited an absorption band centered at a wavelength (λ_{max}^{abs}) of 375 nm (extinction coefficient: 2.32×10^6 M^{-1} cm^{-1}), no apparent absorption band appeared for the original Au NPs having a mean diameter of 2.9 ± 0.5 nm (Figure 2A). On the basis of the well-established spectral assignment for the Au(I) thiolate complexes, we infer that the absorption of Man-Au NDs at 375 nm originates from metal-centered and/or ligand−metal charge transfer (LMCT; S → Au) transitions.[15] The fluorescence bands of the original Au NPs and Man-Au NDs were centered at wavelengths of 618 and 545 nm, respectively (Figure 2B). We note that the fluorescence intensity of the Man-Au NDs was ∼240 000-fold higher than that of the original Au NPs. To ensure that those bands were indeed fluorescence signals, we measured the spectra of Man-Au ND solutions at various concentrations. We observed a linear relationship between the signal intensity and the concentration over the range 0.015−100 nM (R^2 = 0.99) and a limit of detection (LOD) of 10 pM (data not shown). We purified the fluorescent Man-Au NDs by conducting centrifugal filtration (13 500g) for 40 min through a filter having a cutoff of 10 kDa. When compared with that of the original Man-Au NDs solution, the fluorescence of the removed solution at 375 nm was negligible. As a reference, we did not observe any fluorescence of Man-SH (2.5 mM) in 5 mM sodium tetraborate (data not show). The results reveal that the fluorescence is truly from the particles. The quantum yield (QY) of the as-prepared Man-Au NDs was 8.6%, determined through comparison with 10^{-6} M quinine (QY = 53%) shown in Figure S2 in the Supporting Information. This QY is higher than those (QY ≈ 0.001−5%) of the best currently available water-soluble, alkanethiol-protected Au nanoclusters and our previously prepared 11-mercaptoundecanoic acid (11-MUA)-protected Au NDs (11-MUA-Au NDs).[10,16−18] This QY is also comparable to those of Au NDs that are encapsulated and stabilized by such polymers as polyamidoamine (PAMAM) dendrimers and polyethylenimine (PEI);[19] there are, however, problems associated with the general water solubility, difficult bioconjugation, and chemical- and photoinstability of such polymer-protected Au NDs. The fluorescence brightness of our prepared Man-Au ND is stronger than that of polymer stabilized Au NDs, suggesting that our Man-Au ND is more suitable for cell imaging.

At different Man-RSH/Au NPs molar ratios, we obtained differently sized (2.9−1.5 nm) of Man-Au NDs that fluoresced at various wavelengths (618−525 nm), while they all absorbed light at 375 nm (see Supporting Information, Figure S3). The TEM image (Figure S3 in the Supporting Information) reveals that there were no Au NDs present in the solution at the concentration of Man-RSH higher than 20 mM; Au NPs were all dissociated into Au−thiolate complexes. As a result, the as-prepared solution did not absorb light at 375 nm and fluoresce. The sizes of these Au NDs decreased upon increasing the concentration of Man-RSH, resulting from producing significant fragmentation energies; i.e., Au NPs tend to dissociate into smaller Au clusters and Au−thiolate complexes once the Man-RSH molecules adsorbed onto their surfaces.[20] The results further support that the Man-Au NDs fluoresced when excited at 375 nm.

We further studied the behavior of the Man-Au NDs through measurements of their fluorescence lifetime. By fitting to a biexponential fluorescence decay, we obtained lifetimes t_1 and t_2 for the Man-Au NDs of 159 and 834 ns, respectively (see the Supporting Information, Figure S4). There are several explanations of the photoluminescence properties of Au clusters. The interband (d-band electrons to the sp-conduction band) and the relaxed radiative recombination across the HOMO−LUMO gap

(15) (a) Forward, J. M.; Bohmann, D., Jr.; Staples, R. *J. Inorg. Chem.* **1995**, *34*, 6330–6336. (b) Yam, V. W.-W.; Lo, K. K.-W. *Chem. Soc. Rev.* **1999**, *28*, 323–334. (c) Yam, V. W.-W.; Cheng, E. C.-C.; Zhou, Z.-Y. *Angew. Chem., Int. Ed.* **2000**, *39*, 1683–1685. (d) Yam, V. W.-W.; Cheng, E. C.-C.; Cheung, K.-K. *Angew. Chem., Int. Ed.* **1999**, *38*, 197–199.

(16) (a) Wyrwas, R. B.; Alvarez, M. M.; Khoury, J. T.; Price, R. C.; Schaaff, T. G.; Whetten, R. L. *Eur. Phys. J. D* **2007**, *43*, 91–95. (b) Negishi, Y.; Nobusada, K.; Tsukuda, T. *J. Am. Chem. Soc.* **2005**, *127*, 5261–5270. (c) Link, S.; Beeby, A.; FitzGerald, S.; El-Sayed, M. A.; Schaaff, T. G.; Whetten, R. L. *J. Phys. Chem. B* **2002**, *106*, 3410–3415. (d) Negishi, Y.; Tsukuda, T. *Chem. Phys. Lett.* **2004**, *383*, 161–165. (e) Price, R. C.; Whetten, R. L. *J. Am. Chem. Soc.* **2005**, *127*, 13750–13751. (f) Schaaff, T. G.; Shafigullin, M. N.; Khoury, J. T.; Vezmar, I.; Whetten, R. L. *J. Phys. Chem. B* **2001**, *105*, 8785–8796.

(17) (a) Wang, G.; Huang, T.; Murray, R. W.; Menard, L.; Nuzzo, R. G. *J. Am. Chem. Soc.* **2005**, *127*, 812–813. (b) Huang, T.; Murray, R. W. *J. Phys. Chem. B* **2001**, *105*, 12498–12502. (c) Wang, G.; Guo, R.; Kalyuzhny, G.; Choi, J.-P.; Murray, R. W. *J. Phys. Chem. B* **2006**, *110*, 20282–20289. (d) Yang, Y.; Chen, S. *Nano Lett.* **2003**, *3*, 75–79. (e) Link, S.; El-Sayed, M. A.; Schaaff, T. G.; Whetten, R. L. *Chem. Phys. Lett.* **2002**, *356*, 240–246. (f) Bigioni, T. P.; Dag, Ö.; Whetten, R. L. *J. Phys. Chem. B* **2000**, *104*, 6983–6986. (g) Liu, X.; Li, C.; Xu, J.; Lv, J.; Zhu, M.; Guo, Y.; Cui, S.; Liu, H.; Wang, S.; Li, Y. *J. Phys. Chem. C* **2008**, *112*, 10778–10783.

(18) Huang, C.-C.; Chiang, C.-K.; Lin, Z.-H.; Lee, K.-H.; Chang, H.-T. *Anal. Chem.* **2008**, *80*, 1497–1504.

(19) (a) Zheng, J.; Zhang, C.; Dickson, R. M. *Phys. Rev. Lett.* **2004**, *93*, 077402. (b) Zheng, J.; Nicovich, P. R.; Dickson, R. M. *Annu. Rev. Phys. Chem.* **2007**, *58*, 409–431. (c) Tran, M. L.; Zvyagin, A. V.; Plakhotnik, T. *Chem. Commun.* **2006**, 2400–2401. (d) Shi, X.; Ganser, T. R.; Sun, K.; Balogh, L. P., Jr. *Nanotechnology* **2006**, *17*, 1072–1078. (e) Triulzi, R. C.; Micic, M.; Giordani, S.; Serry, M.; Chiou, W.-A.; LeBlanc, R. M. *Chem. Commun.* **2006**, 5068–5070. (f) Duan, H.; Nie, S. *J. Am. Chem. Soc.* **2007**, *129*, 2412–2413.

(20) (a) Krüger, D.; Fuchs, H.; Rousseau, R.; Marx, D.; Parrinello, M. *J. Chem. Phys.* **2001**, *115*, 4776–4786. (b) Konôpka, M.; Rousseau, R.; Štich, I.; Marx, D. *J. Am. Chem. Soc.* **2004**, *126*, 12103–12111.

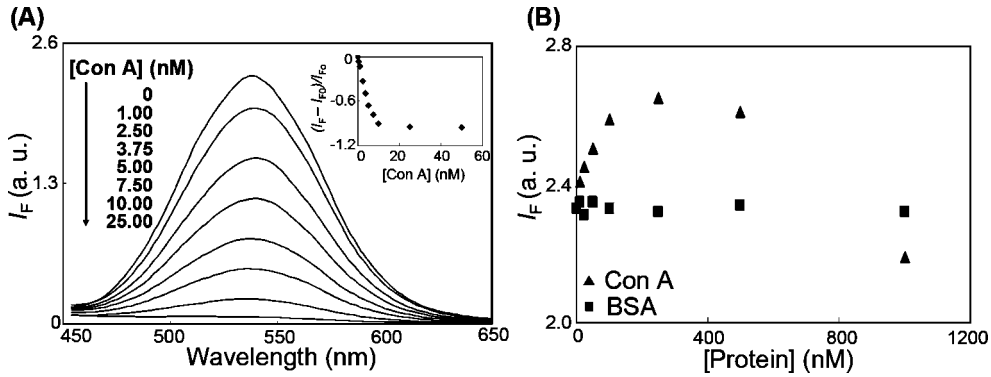

Figure 3. (A) Validation of the use of Man-Au NDs as probes for the detection of Con A. (B) Plots of the fluorescence intensity of Man-Au NDs at 545 nm versus the concentrations Con A and BSA. Inset to part A: Plot of the relative fluorescence $[(I_F - I_{F0})/I_{F0}]$ of the supernatant of the mixture of Con A/Man-Au NDs.

within the sp-conduction band, singlet (fluorescence) and triplet (phosphorescence) excited-state of the molecular-type cluster, often show the monotonic absorbance decline from 200 to 800 nm and exhibit fluorescence >650 nm.[16,17] Recently, more observation of the insensitivity of luminescence wavelengths to the core sizes can explain the luminescence contributions from surface characteristics.[15−17] As particle size decreases, the surface to-volume ratio increases and a larger fraction of the nanoparticle core atoms becomes involved in forming bonds with the core-capping ligands. On the basis of the well-established spectral assignment for the Au(I) thiolate complexes, we infer that the absorption of Man-Au NDs at 375 nm originates from metal-centered and/or ligand−metal charge transfer (LMCT; S → Au) transitions.[15] In addition, our fluorescent Man-Au NDs had large Stokes-shifted fluorescence (1.03 eV) with long lifetimes (t_1/t_2) of 159/834 ns, which is general characteristics of thiol−Au(I) complexes that display ligand−metal charge transfer and metal(I)−metal(I) interactions.[15,21] Thus, we suspect that the fluorescence of our RS-Au NDs was mainly originated from Au ND/polynuclear Au(I)−thiol (core/shell) complexes.[16d,22] The shell of polynuclear Au(I)−thiol suggests that the emission arises from a low-lying triplet state (phosphorescence), populated via intersystem crossing from the lowest singlet state.[16d] We further compared the emission peaks of our the luminescent Man-Au NDs with those of reported monolayer-protected gold clusters.[16,17] The emission peak of Man-Au NDs (λ = 545 nm) was located at an energy higher than those of the Au_{28}(glutathione)$_{16}$ clusters and dodecanethiolate-protected Au_{38} clusters (<1.5 nm).[16c,17f] The blue shift in the emission maxima with the reduction of the cluster sizes is known in terms of the increase in the energy gaps between the quantized levels, d-type core electron to unfilled sp conduction orbitals (interband transitions), ascribed to the smaller core sizes as well as the higher coverage of thiolates and capped molecules like phosphine.[17] In contrast, the λ value for Man-Au NDs (1.8 nm) was inconsistent with those clusters, presumably due to the existence of the outermost layer of Au(I)thiolate complexes.[16d,21,22]

In comparison, the lifetimes for our previous prepared 11-MUA-Au NDs were 48 and 340 ns, respectively.[10,18] The longer lifetimes of the Man-Au NDs are consistent with their stronger fluorescence and smaller size in comparison to those of the 11-MUA-Au NDs. Because the fluorescent Man-Au NDs possess long fluorescence lifetimes, they have great potential for sensing molecules of interest using time-resolved fluorescence. From a practical point of view, it is important to test the stability of the as-prepared Man-Au NDs solution under physiological conditions. The Man-Au NDs were stable when resuspended in sodium phosphate solutions (pH 7.4) containing NaCl at the concentrations up to 1.5 M (see the Supporting Information, Figure S5). Figure S5 in the Supporting Information indicates that the fluorescence intensity of the Man-Au NDs increased upon increasing the pH from 3.0 to 11.0. Slight aggregation of the Man-Au NDs and hydrolysis of the mannose units are the main reasons for the low fluorescence intensities at low pH.

"Turn-Off" Sensor for Detection of Con A. We used the fluorescent Man-Au NDs to test the detection of Con A, a member of the lectin family that selectively binds to α-mannopyranosyl and α-glucopyranosyl residues.[23] Con A exists predominantly as a tetramer of four identical subunits (each ~26 000 Da) at neutral and alkaline pH.[23] We added different amounts of Con A into a sodium phosphate buffer (10 mM, pH 7.0) containing the Man-Au NDs (10 nM), $MnCl_2$ (0.1 mM), and $CaCl_2$ (0.1 mM).[23d] To minimize precipitation and collisions causing fluorescence quenching, the mixed solution with various concentrations of Con A (0−50 nM) were incubated for 60 min and then centrifuged (RCF 20 000*g*, 20 min) prior to fluorescence measurement. In this case, the recorded fluorescence intensities of the supernatants were inversely proportional to the concentrations of Con A (Figure 3A). When the concentration of Con A was greater than 25 nM, after centrifugation we observed (by the naked eye) green pellets of a Con A−Man-Au ND complex under UV lamp illumination, supporting the notion of Con A-induced aggregation of the Man-Au NDs. As a result of

(21) Vogler, A.; Kunkely, H. *Coord. Chem. Rev.* **2001**, *219−221*, 489–507.
(22) (a) Whetten, R. L.; Price, R. C. *Science* **2007**, *318*, 407–408. (b) Schaaff, T. G.; Whetten, R. L. *J. Phys. Chem. B* **2000**, *104*, 2630–2641. (c) Walter, M.; Akola, J.; Lopez-Acevedo, O.; Jadzinsky, P. D.; Calero, G.; Ackerson, C. J.; Whetten, R. L.; Grönbeck, H.; Häkkinen, H. *Proc. Natl. Acad. Sci. U.S.A.* **2008**, *105*, 9157–9162. (d) Jadzinsky, P. D.; Calero, G.; Ackerson, C. J.; Bushnell, D. A.; Kornberg, R. D. *Science* **2007**, *318*, 430–433. (e) Grönbeck, H.; Walter, M.; Häkkinen, H. *J. Am. Chem. Soc.* **2006**, *128*, 10268–10275. (f) Heaven, M. W.; Dass, A.; White, P. S.; Holt, K. M.; Murray, R. W. *J. Am. Chem. Soc.* **2008**, *130*, 3754–3755. (g) Akola, J.; Walter, M.; Whetten, R. L.; Häkkinen, H.; Grönbeck, H. *J. Am. Chem. Soc.* **2008**, *130*, 3756–3757.
(23) (a) Wang, J. L.; Cunningham, B. A.; Edelman, G. M. *Proc. Natl. Acad. Sci. U.S.A.* **1971**, *68*, 1130–1134. (b) Senear, D. F.; Teller, D. C. *Biochemistry* **1981**, *20*, 3076–3083. (c) Cairo, C. W.; Gestwicki, J. E.; Kanai, M.; Kiessling, L. L. *J. Am. Chem. Soc.* **2002**, *124*, 1615–1619 (d) Mn^{2+} and Ca^{2+} must be present for saccharide binding of Con A.

Downloaded by NATIONAL TAIWAN UNIV on July 30, 2009
Published on January 2, 2009 on http://pubs.acs.org | doi: 10.1021/ac8010654

aggregation of the Man-Au NDs, the fluorescence intensities of the supernatants decreased upon increasing the concentration of Con A. We obtained a linear relationship for $[(I_F - I_{F0})/I_{F0}]$ against the concentration of Con A over the range 1.0−10.0 nM ($R^2 = 0.95$), where I_{F0} and I_F are the fluorescence intensities of the Man-Au NDs in the absence and presence of Con A, respectively. The limit of detection (LOD) for Con A was 0.7 nM, based on a signal-to-noise ratio (S/N) of 3; which is comparable to the best reported result.[24]

We obtained a biphasic curve of the fluorescence intensities of the Man-Au NDs solutions at 545 nm against the concentrations of Con A over the range 0−1000 nM (Figure 3B) without centrifugation. At low Con A concentrations (<250 nM), Man-Au NDs−lectin aggregates were formed through specific interactions between the carbohydrate units and the multivalent lectins. The fluorescence intensity of the Man-Au NDs increased initially upon increasing the concentration of Con A over the range 0−250 nM. Con A minimized the interaction of the Man-Au NDs with quenchers present in solution, thereby increasing their fluorescence.[18] When the concentration of Con A was sufficiently high (>250 nM) to induce a greater degree of interparticle cross-linking, precipitation occurred, resulting in a decrease in fluorescence.[6c] A control experiment revealed no obvious change in the fluorescence intensity of the Man-Au NDs in the presence of bovine serum albumin (BSA) (Figure 3B). Even at low Con A concentrations, however, the linearity of the fluorescence intensity of the Man-Au NDs was poor because of precipitation and collisions causing fluorescence quenching.[6]

Selectivity and Inhibition Assays. To test the specificity of this assay toward Con A, we incubated aliquots of the Man-Au ND solutions (10 nM) separately with Con A, some possible interfering proteins (BSA, trypsin inhibitor, β-lactalbumin, carbonic anhydrase, catalase, lysozyme, trypsinogen, conalbumin, myoglobin, insulin, transferrin, and ribonuclease A), and other lectins (DBA from *Dolichos biflorus*, BS-I from *Bandeiraea simplicifolia*, MAA from *Maackia amurensis*, WGA from *Triticum vulgaris*, LcH from *Lens culinaris*, SNA from *Sambucus nigra*, ECA from *Erythrina cristagalli*, and PSA from *Pisum sativum*). Apart from LcH and PSA, which are mannose-binding lectins, the changes in the fluorescence of the Man-Au ND solutions in the presence of the interfering proteins and the tested lectins were all negligible relative to that in the presence of Con A (parts A and B of Figure 4). Relative to LcH and PSA, Con A caused a larger fluorescence change, mainly because of its four binding sites, larger molecular weight (102 kDa), and higher binding affinity toward the Man-Au NDs. The Man-Au NDs sensor allowed us to detect Con A at concentrations as low as 1.0 nM in the presence of a 10 000-fold higher concentration (i.e., 10 μM) of BSA (Figure 4C). Thus, this highly specific sensor has great potential for use in detecting Con A in complex real samples.

Next, we developed binding inhibition assays based on decreasing the binding efficiency between Con A (100 nM) and the Man-Au NDs (10 nM) separately in the presence of the carbohydrates mannose, glucose, galactose, and lactose (each at concentrations in the range 0−225 mM). We observed increased fluorescence of the Man-Au NDs in the supernatants when

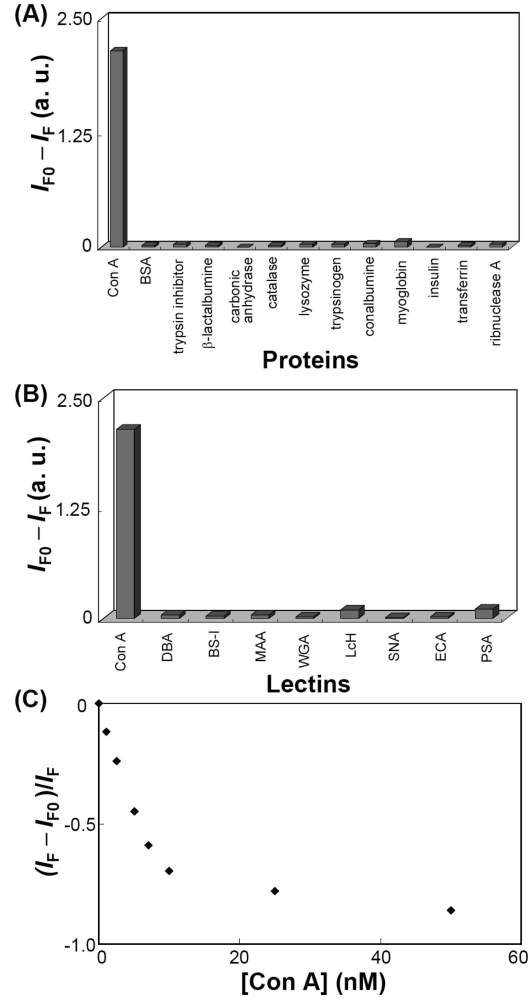

Figure 4. (A, B) Fluorescence changes of the Man-Au ND probe toward Con A, (A) other proteins, and (B) lectins. (C) Plots of the relative fluorescence intensities $[(I_F - I_{F0})/I_{F0}]$ of solutions of the Man-Au ND probe (10 nM) and Con A (0−50 nM) in the presence of 10 μM BSA. Buffer: 10 mM sodium phosphate (pH 7.0) containing 0.1 mM $MnCl_2$ and $CaCl_2$. Other conditions were the same as those described in Figure 3.

mannose and glucose were present at 10 and 75 mM, respectively, revealing that these two carbohydrates can inhibit the Con A-induced aggregation of the Man-Au NDs (Figure 5), albeit at concentrations of 1.0×10^6 and 7.5×10^6 times, respectively, that of Man-Au NDs (10 nM). In contrast, galactose and lactose did not affect the binding of Con A to the Man-Au NDs, even when their concentrations were greater than 225 mM. The inset to Figure 5 displays the linear relationships ($R^2 > 0.94$) between the fluorescence intensity of the supernatants at 545 nm and the mannose and glucose concentrations over the ranges 10−50 and 75−200 mM, respectively. These results are consistent with previous reports that Con A has higher affinity toward mannose than toward glucose.[25] In addition, the multivalent mannose ligands of these Man-Au NDs have a 6-orders-of-magnitude higher affinity for Con A than do the monovalent mannose ligands.

(24) Guo, C.; Boullanger, P.; Jiang, L.; Liu, T. *Biosens. Bioelectron.* **2007**, *22*, 1830–1834.

(25) (a) Sato, K.; Anzai, J.-I. *Anal. Bioanal. Chem.* **2006**, *384*, 1297–1301. (b) Mandal, D. K.; Kishore, N.; Brewer, C. F. *Biochemistry* **1994**, *33*, 1149–1156.

Downloaded by NATIONAL TAIWAN UNIV on July 30, 2009
Published on January 2, 2009 on http://pubs.acs.org | doi: 10.1021/ac8010654

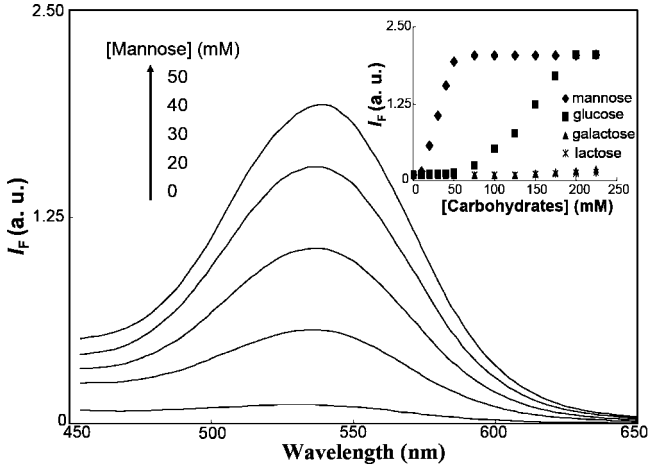

Figure 5. Fluorescence spectra of a solution of Man-Au NDs (10 nM) and Con A (100 nM) in the presence of increasing concentrations of mannose. Inset: Plots of fluorescence intensities (545 nm) of solutions of Man-Au NDs and Con A in the presence of mannose, glucose, galactose, and lactose. Other conditions were the same as those described in Figure 4.

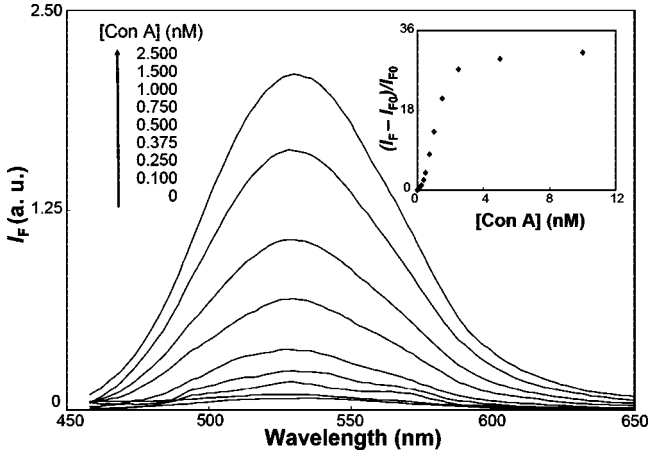

Figure 6. Fluorescence spectra recorded after using the Man-Au NDs (1.0 nM) to selectively enrich the detection of Con A. Inset: Relative fluorescence $[(I_F - I_{F0})/I_{F0}]$ at 545 nm of the resuspended solutions of the mixture of Man-Au NDs (1.0 nM) and Con A (0−10.0 nM). Other conditions were the same as those described in Figure 4.

"Turn-On" Sensor by NP-Assisted Protein Enrichment. We employed a NP-assisted protein enrichment method to further improve the sensitivity of the Man-Au NDs toward ConA.[26] Mixtures (1 mL) of Con A (0−10.0 nM) and Man-Au NDs (1.0 nM) in buffer (10 mM sodium phosphate, 0.1 mM $MnCl_2$ and $CaCl_2$, pH 7.0) were left at room temperature for 60 min. The samples were then centrifuged and the supernatants removed. The precipitates were resuspended in a buffer (pH 7.0, 100 μL) containing 10 mM sodium phosphate, 0.1 mM $MnCl_2$, 0.1 mM $CaCl_2$, and 100 mM mannose and then equilibrated for another 60 min. Figure 6 displays the fluorescence spectra of the resulting Con A solutions. Unlike the situation in Figure 3B, the sensing in

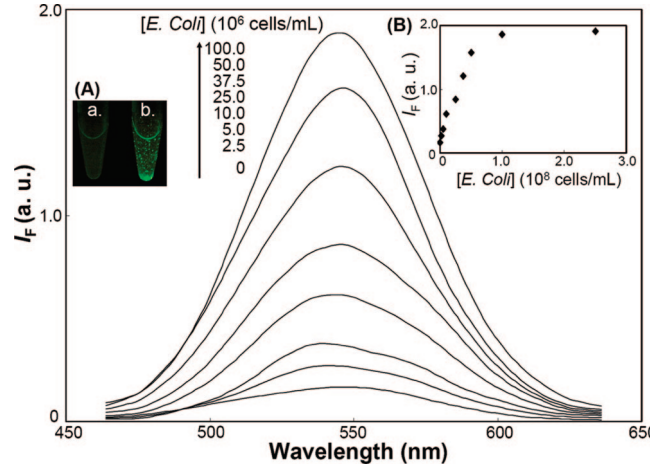

Figure 7. Fluorescence spectra of Man-Au NDs (25 nM) used as probes for the detection of *E. coli* ($(2.50 \times 10^6)-(1.00 \times 10^8)$ cells/mL). (Inset A): Visualization of Man-Au NDs (25 nM) in the (a) absence and (b) presence of *E. coli* (2.50×10^8 cells/mL) upon excitation (365 nm) under a hand-held UV lamp. (Inset B): Plot of fluorescence intensity (545 nm) versus *E. coli* concentration. Other conditions were the same as those described in Figure 4.

Figure 6 reveals a turn-on response: the fluorescence increases upon increasing the Con A concentration. The relationship between the signal enhancement ratio $[(I_F - I_{F0})/I_{F0}]$ and the Con A concentration (inset to Figure 6) was linear from 0.1 to 1.5 nM ($R^2 = 0.96$), with the LOD (at a S/N ratio of 3) for Con A being 75 pM. Thus, the Man-Au ND-assisted Con A enrichment process provided a nearly 1 order greater sensitivity improvement relative to that in Figure 3A. To the best of our knowledge, this approach provided the lowest LOD value (75 pM) for Con A when compared to the other nanomaterials-based detecting method.[5,6,24]

***E. coli* Labeling by Fluorescent Man-Au NDs.** Type 1 fimbriae present on the surface of Enterobacteriaceae, such as *E. coli*, are responsible for their mannose- and mannoside-binding activities.[27,28] Thus, we investigated whether our Man-Au NDs had the capability of binding mannose-specific adhesin FimH of type 1 pili in *E. coli* and, therefore, whether they could be used to detect *E. coli*. Type 1 pili are filamentous proteinaceous appendages that extend from the surface of many Gram-negative organisms; they are composed of FimA, FimF, FimG, and FimH proteins.[27] FimA accounts for more than 98% of the pilus protein; FimH is uniquely responsible for the binding to D-mannose.[28] In this study, we tested an *E. coli* strain K12 (ATCC 25404) that expresses wild-type 1 pili. After incubation of the bacterial suspensions $((1.00 \times 10^6)-(2.50 \times 10^8)$ cells/mL, 1.0 mL) with the Man-Au NDs (25 nM) in phosphate-buffered saline (PBS, pH 7.4) at 25 °C for 60 min, we centrifuged the suspensions at RCF 10 000*g* for 20 min. Incubation with *E. coli* (2.50×10^8 cells/mL) revealed that the Man-Au NDs (25 nM) bind to the bacteria, yielding brightly fluorescent cell clusters (Figure 7, inset A). The supernatant solution containing unbound Man-Au NDs was discarded, and the cells were washed twice with PBS. *E. coli* bacteria labeled with the Man-Au NDs fluoresced with a

(26) (a) Zheng, M.; Huang, X. *J. Am. Chem. Soc.* **2004**, *126*, 12047–12054. (b) Kong, X. L.; Huang, L. C. L.; Hsu, C.-M.; Chen, W.-H.; Han, C.-C.; Chang, H.-C. *Anal. Chem.* **2005**, *77*, 259–265. (c) Huang, Y.-F.; Chang, H.-T. *Anal. Chem.* **2006**, *78*, 1485–1493. (d) Huang, C.-C.; Chiu, S.-H.; Huang, Y.-F.; Chang, H.-T. *Anal. Chem.* **2007**, *79*, 4798–4804.

(27) Soto, G. E.; Hultgren, S. J. *J. Bacteriol.* **1999**, *181*, 1059–1071.

(28) (a) Harris, S. L.; Spears, P. A.; Havell, E. A.; Hamrick, T. S.; Horton, J. R.; Orndorff, P. E. *J. Bacteriol.* **2001**, *183*, 4099–4102. (b) Krogfelt, K. A.; Bergmans, H.; Klemm, P. *Infect. Immun.* **1990**, *58*, 1995–1998.

Downloaded by NATIONAL TAIWAN UNIV on July 30, 2009
Published on January 2, 2009 on http://pubs.acs.org | doi: 10.1021/ac8010654

green color. The bacteria pellets were then resuspended in PBS containing 100 mM mannose, which displaced the Man-Au NDs from the surfaces of the *E. coli*. After centrifugation, we measured the fluorescence of the supernatants. Figure 7 indicates that the fluorescence increased upon increasing the concentration of *E. coli*. The relationship between the fluorescence signal and the *E. coli* concentration (Figure 7, inset B) was linear from 1.00×10^6 to 5.00×10^7 cells/mL ($R^2 = 0.96$), with the LOD (at a S/N ratio of 3) of *E. coli* being 7.20×10^5 cells/mL. Most conventional methods (e.g., plating and culturing, biochemical tests, microscopy, flow cytometry, luminescence) for the detection of bacteria are time-consuming to obtain the results. Although much faster detection methods are becoming available (e.g., immunosensors, DNA chips), they have failed to gain wide acceptance because of the high user expertise required, the high cost of labeling reagents, and the low stability of antibodies and DNA recognition elements. Recently, silica-coated magnetic NPs after being conjugated with mannose have been demonstrated easily for detection of Con A and *E. coli* with a high capture efficiency of 65% in just 5 min.[2b] However, Con A and *E. coli* need to be labeled with fluorescein and PicoGeen dye, respectively. In addition, our fluorescent Man-Au NDs are easily prepared than that of the bioconjugated silica-coated magnetic NPs.

CONCLUSION

We have devised a novel, simple, and convenient method for the preparation of water-soluble biofunctional Au NDs for the detection of lectin. Our fluorescent Man-Au NDs are easily purified and are capable of sensing, under optimal conditions, Con A with high sensitivity (LOD = 75 pM) and remarkable selectivity over other proteins and lectins. Furthermore, we have also developed a new method for fluorescence detection of bacteria using these water-soluble Man-Au NDs. Incubation with *E. coli* revealed that the Man-Au NDs bind to the bacteria, yielding brightly fluorescent cell clusters. This aggregation is due to the multivalent interactions between the mannosylated Au NDs and mannose receptors located on the bacterial pili. In contrast to standard methods for pathogen detection, which require up to 2 days for analysis, our fluorescent carbohydrate-functionalized Au NDs allow of the presence of *E. coli* to be detected in as little as 3 h. To the best of our knowledge, this paper provides the first example of the use of fluorescent Au NDs for the sensing both lectins and bacteria.

ACKNOWLEDGMENT

This study was supported by the National Science Council of Taiwan under Contracts NSC 95-2113-M-002-026-MY3, NSC 97-2627-M-002-010, and NSC 97-2627-M-002-011.

SUPPORTING INFORMATION AVAILABLE

Additional information as noted in text. This material is available free of charge via the Internet at http://pubs.acs.org.

Received for review May 26, 2008. Accepted December 1, 2008.

AC8010654

Downloaded by NATIONAL TAIWAN UNIV on July 30, 2009
Published on January 2, 2009 on http://pubs.acs.org | doi: 10.1021/ac8010654